ARTICLE NO. 78-1318

Fault Detection Threshold Determination Technique Using Markov Theory

Bruce K. Walker* and Eliezer Gai†
C.S. Draper Laboratory, Inc., Cambridge, Mass.

A method for determining time-varying Failure Detection and Identification (FDI) thresholds for single-sample decision functions is described in the context of a triplex system of inertial platforms. A cost function consisting of the probability of vehicle loss due to FDI decision errors is minimized. A discrete Markov model is constructed from which this cost can be determined as a function of the decision thresholds employed to detect and identify the first and second failures. Optimal thresholds are determined through the use of parameter optimization techniques. The application of this approach to threshold determination is illustrated for the Space Shuttle's inertial measurement instruments.

Introduction

THE current trend in aerospace system design is the inclusion of redundancy of critical sensors to enhance the overall control system reliability. The excess number of instruments can be exploited to preclude the use of bad data in a passive way (e.g. selection filter), an active way (e.g. Failure Detection and Identification [FDI] system), or both. Selection techniques are often of the midvalue type.[1] In contrast, several different approaches exist for implementing an FDI algorithm.[2-4] This paper shall be limited to FDI algorithms that are based on comparison tests among like sensor outputs, although the method discussed can be generalized to include BITE (Built-In Test Equipment) as well. The method will also be constrained to single-sample tests, thereby disregarding the more sophisticated case of sequential tests.

Classical detection theory[5] cannot be used directly in failure detection problems for several reasons. One major difficulty is that the magnitude of a bias failure is usually completely unknown a priori. This problem can be solved in an efficient manner using a sensitivity approach[6,7] which predicts those failure magnitudes that are likely to cause violation of the mission requirements. This approach can be modified to reflect any prior distribution of failure magnitudes that exist, if such information is available. For the application considered here and for most cases of interest, failure magnitude information is unavailable. Therefore, the assumption has been made that the failure magnitude may take any value with equal likelihood. Another problem is that an on-line failure detection algorithm is a dynamic process so that its design must take into account such dynamic effects as time-varying measurement statistics and the cumulative effect of the probabilities of error. A Markov model will be used here to describe the dynamics of the FDI process.

Any FDI algorithm is composed of two stages: 1) data processing to form a decision function, and 2) comparison to a threshold as the decision mechanism. It is assumed here that the decision function is in its simplest form, namely a direct comparison between the outputs of like components. The problem to be addressed is the method in which time-varying thresholds can be determined to minimize a cost function for given detection and isolation decision functions. A Markov model which includes all the possible states of the system is constructed. The single-step probability transition matrix for this model is a function of all the time-varying FDI thresholds via the per test probabilities of decision errors. One of the states in this model is defined as vehicle loss, wherein the control system must use the output of a failed sensor due to either a lack of unfailed instruments or some sequence of errors by the FDI system. The probability that this state is the state of the system becomes the cost function to be minimized. The functional form of the threshold is predetermined and a gradient method is used to optimize the defining parameters.

This method is applied to the determination of the time-varying thresholds used for FDI of the three Inertial Measurement Units (IMU's) onboard the Space Shuttle for a typical entry phase mission. The advantages of this method over the popular 3σ method[8,9] for threshold determination are also discussed.

Methodology

Cost Function

The primary objective of a FDI system is to increase the likelihood that the navigation, guidance, and flight control systems will satisfactorily complete the objectives of the mission. Therefore, an apt choice for a cost function reflecting the performance of the FDI system is the probability of vehicle loss[10] denoted P_{vl}. A vehicle loss is said to occur when, due to some sequence of sensor failures and FDI decision errors, the navigation system is forced to utilize data from failed sensors. A sensor is deemed failed when its measurements are corrupted by a bias error sufficiently large to cause violation of the mission requirements if its output is used in the navigation computations. Otherwise, the sensor is considered good. Thus, P_{vl} represents the probability that the Redundancy Management (RM) system will be unsuccessful in preventing the use by the navigation system of data from failed sensors. This probability depends upon the failure probabilities of the instruments of interest (denoted P_f) and the probabilities of the various possible FDI decision outcomes. These probabilities will be referred to as the FDI performance probabilities.

In general, a FDI algorithm is executed in two stages—the detection stage and the isolation stage. The former is used to test for the presence of a failure and, if such a test is positive, triggers the latter in an effort to specifically identify the faulty component. A separation then exists between the detection and isolation tasks. It is assumed here that the two stages are independent, although this need not be true for application of

Presented as Paper 78-1318 at the AIAA Guidance and Control Conference, Palo Alto, Calif., Aug. 7-9, 1978; submitted Aug. 28, 1978; revision received Jan. 8, 1979.

Index categories: Spacecraft Navigation, Guidance, and Flight Path Control; Sensor Systems; Reliability, Maintainability, and Logistics Support.

*Draper Fellow, Student, Massachusetts Institute of Technology, Department of Aeronautics and Astronautics. Student Member, AIAA.

†Staff Engineer, Control and Flight Dynamics Division.

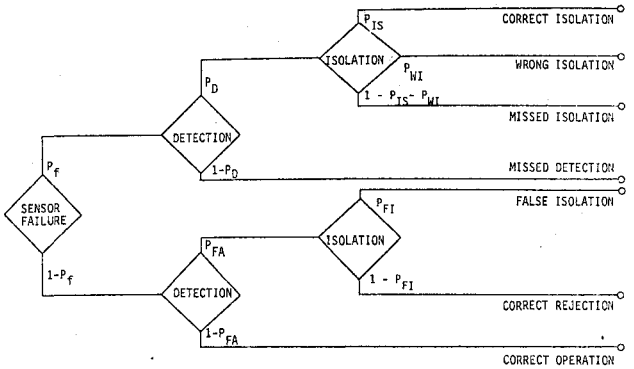

Fig. 1 FDI decision tree.

the method, provided the statistical correlation between the two stages can be quantified. Let three-level represent an operating condition where the FDI system is indicating that three instruments are operating normally, and similarly for two-level and one-level. For systems employing triplets of like instruments, the performance probabilities are then defined as follows:

P_{FA3} = Pr[false alarm (or Type I) error by the three-level detection logic]

P_{M3} = Pr[missed alarm (or Type II) error by the three-level detection logic]

P_{FA2} = Pr[false alarm error by the two-level detection logic]

P_{M2} = Pr[missed alarm error by the two-level detection logic]

P_{FI} = Pr[isolation decision by the two-level isolation logic given the occurrence of a false alarm]

P_{IS} = Pr[correct isolation decision by the two-level isolation logic given detection]

P_{WI} = Pr[incorrect isolation decision by the two-level isolation logic given detection]

No three-level isolation error probabilities are included because it is assumed that the majority voting technique is used for isolation. Since this isolation technique employs no threshold, an isolation decision always follows a detection. It is further assumed that the probability of incorrect isolation at this level is negligible because it is smaller than the product $P_f P_{FA3}$.

If the probability density functions (pdf's) of the decision functions are completely known for both the normal and failed modes, then the performance probabilities become functions of just the thresholds. These pdf's can be found using the sensitivity method of Refs. 6 and 7. In general, these pdf's may be time-varying thereby implying that the implementation of time-varying thresholds might enhance the system performance. In either case, the performance probabilities become implicit functions of time. The next section will indicate that P_{vl} is a function only of the performance probabilities and hence can be minimized by selection of the threshold form.

Markov Model

It was mentioned previously that this paper deals only with FDI systems employing single-sample tests. It will be assumed that the outcomes of successive FDI tests are independent. Under this assumption, a discrete-state Markov chain can be used to describe the time evolution of the system state.[10]

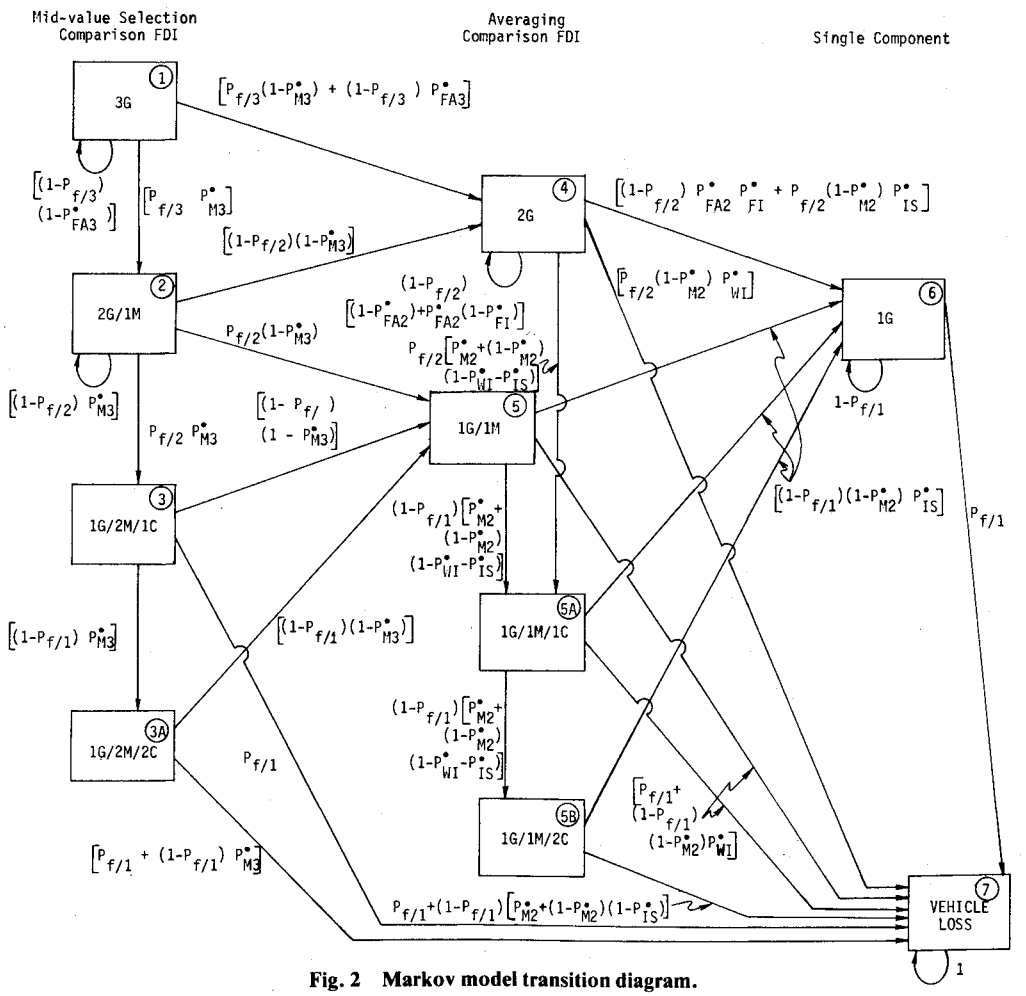

Fig. 2 Markov model transition diagram.

Each possible state of the system is characterized by 1) the number of good components still available for use in navigation (denoted G), 2) the number of failed components not yet identified by the FDI system as failed (i.e. missed) and therefore still available for use in navigation (denoted M), and 3) the number of components eliminated from consideration by the FDI system. It is assumed that once a sensor has been declared failed by the FDI logic, it is removed from future consideration. This assumption can be relaxed if the technique for recovering instruments previously declared failed can be represented in a probabilistic sense. This relaxation would have the effect of making it possible under certain circumstances to recover from a vehicle loss and is not considered here.

Considering a single FDI test, a decision tree as in Fig. 1 can be constructed to represent the possible outcomes for each state. Note that when considering a three-level state, the "wrong isolation," "missed isolation," and "correct rejection" branches of the decision tree of Fig. 1 are not present because majority voting is used for three-level isolation. It is assumed that simultaneous failures occur with negligible probability (order of P_f^2). It can be seen from Fig. 1 that the probabilities of the various outcomes are functions of the probability of a sensor failure during the interval between FDI tests P_f and the performance probabilities.

Construction of the decision tree for each possible system state results in the Markov transition diagram shown as Fig. 2. The probabilities of the possible one-step transitions are indicated on the figure. The probability of the occurrence of a sensor failure during a single FDI time interval when i good sensors are operating is denoted $P_{f/i}$. Included in the diagram are three transient substates labelled 3A, 5A, and 5B. These are included because it is not desirable for the system to remain in states 3 or 5 for more than a few consecutive FDI tests. In the case of state 3, the presence of two soft failures might result in the transmission of bad data to the navigation system when a midvalue measurement selection scheme is employed because the two failures might be similar in the affected axes and the polarity. This would also tend to invalidate the assumption made above on the likelihood of three-level isolation errors. In the case of state 5, averaging of the two available measurements for transmission to the navigation system would produce navigation data corrupted by the presence of the bias in the output of the failed instrument. The persistence of these states for three or more consecutive FDI tests is considered a vehicle loss. The limit of three tests employed here was arbitrarily chosen. The use of N as the limit necessitates the addition to the model of $2N-3$ substates of the form of 3A, 5A, and 5B; therefore N should be kept as small as possible. The number of consecutive tests with the same system state is represented by C in the transition diagram.

From Fig. 2, the time-varying one-step probability transition matrix $P(n)$ can be constructed. Let $\pi(n)$ be the vector of probabilities corresponding to each of the possible system states at the nth FDI test. The recursion formula for updating π is then

$$\pi(n+1) = P(n)\pi(n) \tag{1}$$

with some given initial condition $\pi(0)$. The cost P_{vl} is the probability that the system is in the vehicle loss state at the end of the mission and is therefore one of the elements of $\pi(N)$ where N is the total number of FDI tests during the mission.

Note that vehicle loss is a trapping state under the assumptions detailed above. Therefore, the probability that the system state is vehicle loss grows monotonically with the number of FDI tests and hence with time. In some applications there may exist compelling reasons for minimizing this probability at each point in time rather than just its final, and therefore, maximum value. Such an extension is not treated here. Note, however, that the method of solution presented here will lead to a minimax solution of the more general problem because of the monotonicity.

Many techniques exist for accomplishing this task with the most efficient technique generally reflecting the level of complexity of the application. When only a few (1, 2, or perhaps 3) parameters define the thresholds, the minimization can be performed by inspection as in Ref. 6. Otherwise, it is necessary to employ some type of parameter optimization algorithm.

The algorithm chosen for use here is the steepest descent method. By a modification of the well-known formula for the propagation of the state probability vector associated with a Markov chain,[11] one obtains

$$\pi(N) = \left[\prod_{k=1}^{K} P_k{}^{N_k}\right]\pi(0) \tag{2}$$

where the assumption has been made that the thresholds and performance probabilities are constant over each of K subintervals, P_k is the resulting constant one-step probability transition matrix for the kth subinterval and N_k is the number of FDI tests during the kth subinterval. The form of Eq. (2) lends itself to a concise calculation of the cost gradient for use in the steepest descent procedure. The gradient is given by

$$\frac{\partial P_{vl}}{\partial \boldsymbol{P}} = \sum_{k=1}^{K} \frac{\partial P_{vl}}{\partial \boldsymbol{PR}_k} \frac{\partial \boldsymbol{PR}_k}{\partial \boldsymbol{T}_k} \frac{\partial \boldsymbol{T}_k}{\partial \boldsymbol{P}} \tag{3}$$

where

$\boldsymbol{P}$ = parameter vector (to be determined)
$\boldsymbol{PR}_k$ = vector of performance probabilities during the kth subinterval (assumed constant)
$\boldsymbol{T}_k$ = vector of thresholds during the kth subinterval (assumed constant)

A numerical perturbation technique is used to evaluate the first partial derivative in Eq. (3), thereby circumventing the element-by-element expansion of Eq. (2). The second partial derivative involves only the known (often tabular) density functions of the performance probabilities. The last partial derivative is evaluated analytically from the known functional form of the thresholds.

The implementation of the steepest descent algorithm employed in this paper includes a circularization procedure to avoid the "ravine" problem[12] and automatic step size control to aid the convergence. Several initial guesses at the optimal parameters are operated upon to check the global optimality of the results.

Application to Space Shuttle Entry Mission

The method described above will now be applied to determine time-varying thresholds for the FDI of the triplex Inertial Measurement Units (IMU's) on the Space Shuttle Vehicle. The mission to be considered is the first Orbital Flight Test (OFT) mission. The mission is of approximately 45 min duration beginning with a deorbit burn to re-enter from a 120-mile-high orbit and ending with touchdown on the runway at Edwards AFB. For the last 7 min of the mission, the navigation system has radio and air data navigation aids available in the form of TACAN and a barometric altimeter and, for the last 2 min, the Microwave Landing System (MLS) at Edwards. Otherwise, all navigation data are derived from the redundant IMU's.

The IMU FDI system operates at a 0.0625 Hz rate and consists of two independently operating sections, one for accelerometer FDI and one for gyro FDI. In both cases, and for both three-level and two-level, the detection decision function is the squared magnitude of a three-dimensional vector representing the vector difference of the measurements from two of the IMU's. For two-level isolation, the skew geometry of the platforms is exploited.[13] The vector dif-

Table 1 IMU error model (3 σ values)

Accelerometer bias	50 μg
Accelerometer scale factor	141 ppm
Accelerometer IA misalignment	15 arc-s
Accelerometer quantization (1 cm/s)	$1/\sqrt{12}$ cm/s
Gyro bias drift	0.035 deg/h
Gyro g-sensitive drift	
Input axis	0.025 deg/h/g
Spin axis	0.025 deg/h/g
Gyro g^2-sensitive drift	
Input/spin plane	0.025 deg/h/g^2
Spin/output plane	0.025 deg/h/g^2
Input/output plane	0.005 deg/h/g^2
Random gyro drift	0.003 deg/h
Effective resolver error (rss)	40.1 arc-s
Case to nav. base misalignment	100 arc-s
Gimbal nonorthogonalities	50 arc-s

ference used for detection is transformed into the coordinate frame of each of the two operating platforms. In each of these frames, the two components lying in the input plane of the instrument which is used as a two-degree-of-freedom (2 DOF) sensor are squared and added. The remaining single-axis components are also squared. This procedure results in four decision functions, two of the 2 DOF type and two of the single DOF type. When a single bias failure is present, the component(s) of the measurement difference which is (are) orthogonal to the failed axis (axes) are unaffected by the failure. Thus, the two-level isolation logic identifies a failure when exactly three of the four decision functions exceed their thresholds. The identified platform is the one which produces the single decision function that does not exceed its threshold.

By assuming that the components of the decision vectors are uncorrelated and jointly Gaussian with identical variances, approximated by the largest of the three, the decision functions can be approximated by chi-square random variables with the same number of degrees of freedom as of components making up the decision function (3, 2, or 1). The noncentrality parameter for the chi-square distribution is directly related to the magnitude of any failure that might be present.

By performing a covariance analysis for a normal Shuttle IMU, the required statistics are obtained of the vectors from which the decision functions are formed. The IMU error model is presented in Table 1, and the resulting maximum component standard deviation for the accelerometers is shown as Fig. 3. Note that these statistics are time-varying. The piecewise constant approximation to the component statistics is also shown on the figure. For gyros, the approximation is very similar but will not be shown here to conserve space. Using the sensitivity analysis techniques of Refs. 6 and 7, the failure magnitudes that yield the probability of violating the mission requirements in the range (0, 1) can be determined. The results for accelerometers appear in Table 2. Again, the gyro results are similar.

The Type I and Type II error probabilities can now be evaluated as follows. For Type I (or false alarm) errors, the probability of occurrence for a single FDI test is given by

$$P_I(\eta,t) = \int_{\eta}^{\infty} p_N(u,t)\,du \tag{4}$$

where η is the appropriate threshold and $p_N(u,t)$ is the central chi-square pdf given by

$$p_N(u,t) = \frac{1}{2^{n/2}[\sigma(t)]^n \Gamma(n/2)} \exp\left(-\frac{u}{2[\sigma(t)]^2}\right) u^{n/2-1} \tag{5}$$

where n is the number of degrees of freedom, $\sigma(t)$ is the time-varying component standard deviation, and $\Gamma(\cdot)$ is the Gamma function. P_{FA3} and P_{FA2} are evaluated directly from Eq. (4) using $n=3$ and the $\sigma(t)$ for detection. A false isolation at the two-level requires three of the four isolation decision functions to exceed the single isolation threshold. Let α_1 and α_2 be the values of P_I for $n=1$ and $n=2$, respectively, using the isolation value for $\sigma(t)$. Then

$$P_{FI} = \tfrac{1}{2}\alpha_2^2\alpha_1(1-\alpha_1) + \tfrac{1}{2}\alpha_1^2\alpha_2(1-\alpha_2) \tag{6}$$

For Type II (or missed alarm) errors, the error probability for each FDI test is given by

$$P_{II}(\eta,t) = \int_0^{\eta(t)} \left[\int_{-\infty}^{\infty} p(u,t|B)\,p_{MF}(B)\,dB\right] du \tag{7}$$

where $p_{MF}(B)$ is the pdf of the event of violating the mission requirements as a function of the failure magnitude B, which

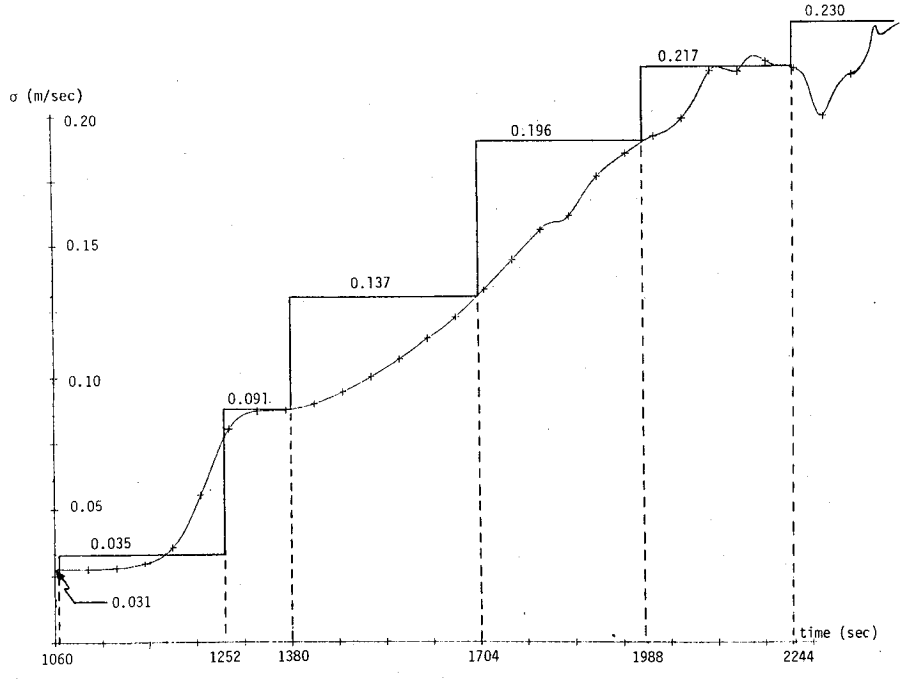

Fig. 3 Actual and piecewise constant approximation to accelerometer standard deviation.

Table 2 Probability of violating mission requirements

Accelerometer bias failure magnitude, m/s^2	Probability of violating mission requirements
0.019999	0.0000
0.020999	0.0000
0.021999	0.0170
0.022999	0.0470
0.023999	0.0848
0.024999	0.1283
0.025999	0.1763
0.026999	0.2278
0.027999	0.2820
0.028999	0.3302
0.029999	0.3959
0.030999	0.4546
0.031999	0.5136
0.032999	0.5725
0.033999	0.6307
0.034999	0.6878
0.035999	0.7432
0.036999	0.7962
0.037999	0.8462
0.038999	0.8923
0.039999	0.9334
0.040999	0.9679
0.041999	0.9931
0.042999	1.0000

is obtained from Table 2 and its counterpart for gyros, and $p(u,t|B)$ is the noncentral chi-square pdf given by

$$p(u,t|B) = \frac{1}{2^{n/2}[\sigma(t)]^n\sqrt{\pi}} \exp\left(-\frac{B^2+u^2}{2[\sigma(t)]^2}\right) u^{(n-2)/2} \cdot \sum_{j=0}^{\infty} \frac{(B^2u)^j \Gamma(j+\frac{1}{2})}{[\sigma(t)]^{4j}(2j)!\,\Gamma(j+n/2)} \tag{8}$$

where again n is the number of degrees of freedom. It should be noted that for any n the sum can be expressed in a closed form.[6,14] P_{M3} and P_{M2} are directly evaluated using Eq. (7) and the detection value for $\sigma(t)$. An incorrect isolation at the two-level occurs when exactly three isolation decision functions exceed the isolation threshold with one threshold excursion due to a Type I error. A correct isolation occurs when the proper three isolation decision functions exceed the isolation threshold. Let β_1 and β_2 be the values of P_{II} for $n=1$ and $n=2$, respectively, using the isolation value for $\sigma(t)$, and assume that failures are equally likely affecting each of the three orthogonal input axes of the instruments. Then

$$P_{IS} = \tfrac{1}{3}(1-\beta_2)(1-\beta_1)[2(1-\beta_2)(1-\alpha_1) + (1-\beta_1)(1-\alpha_2)] \tag{9}$$

$$P_{WI} = \tfrac{1}{3}(\beta_2+\beta_1-2\beta_2\beta_1)[2(1-\beta_2)\beta_1 + \beta_2(1-\beta_1)] \tag{10}$$

As a sample, Figs. 4 and 5 present plots of P_{FA3} and P_{M3} vs the threshold value for two values of time (1060 s and 1988 s after deorbit) for the accelerometers.

It was mentioned previously that the time-varying nature of the decision function statistics leads one to expect that the FDI performance would be enhanced by the use of time-varying thresholds. For the Shuttle IMU's, the specified threshold functional forms are[15]

$$T_3 = T_{2D} = (a+bt)^2$$

$$T_{2I} = (c+dt)^2$$

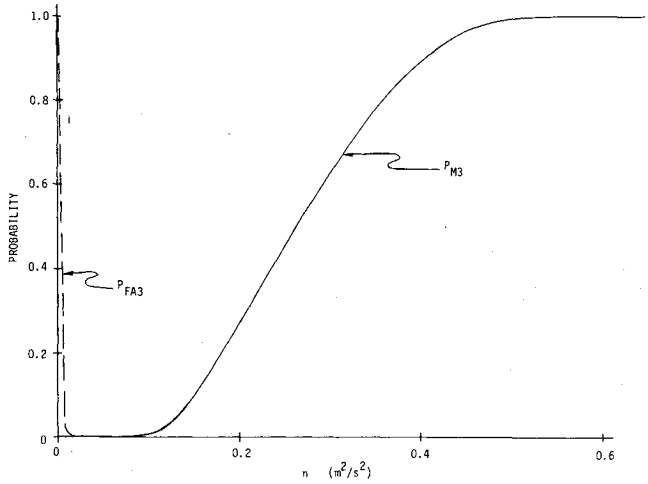

Fig. 4 P_{FA3} and P_{M3} for accelerometers at $t=1060$ s.

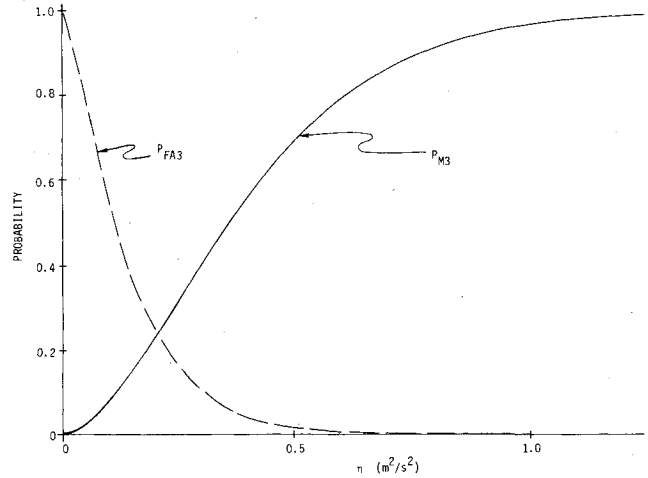

Fig. 5 P_{FA3} and P_{M3} for accelerometers at $t=1998$ s.

where T_3 is the three-level detection threshold, T_{2D} is the two-level detection threshold, and T_{2I} is the two-level isolation threshold. These functional forms are used for both gyro and accelerometer FDI. The parameters to be determined for each sensor type, therefore, are a, b, c, and d.

Application of the optimization procedure of the previous section to the accelerometers produces the results shown in Table 3. As is indicated in the table, it was necessary occasionally to intervene manually in the iterative procedure to aid the convergence of the algorithm. In nearly every case, this intervention merely overcame some convergence difficulty related to the fact that the performance probability functions, since they are not expressable in closed forms, were tabularized for storage in the computer. It should be noted that different initial guesses from the one indicated by Table 3 were tried and the results (not shown here) indicated convergence to the same optimal parameter values. The final accelerometer results are

$$a=0.350\ \text{m/s} \qquad b=4.35\times10^{-4}\ \text{m/s}^2$$

$$c=0.306\text{m/s} \qquad d=2.83\times10^{-4}\ \text{m/s}^2$$

$$P_{vI}=8.89\times10^{-7}$$

Table 4 lists the complete results including the performance probabilities.

Table 3 Optimization results of acceleration threshold

Pass	a, m/s	b, 10^{-4} m/s^2	c, m/s	d, 10^{-4} m/s^2	P_{VL}
1	0	5.00	0.050	4.000	1.187×10^{-3}
2	0	4.00	0.070	3.000	1.023×10^{-3}
3[a]	0.280	2.00	0.280	1.300	7.057×10^{-5}
4	0.280	2.42	0.280	1.216	2.651×10^{-5}
5	0.280	2.59	0.280	1.191	1.673×10^{-5}
6	0.280	2.71	0.280	1.178	9.622×10^{-6}
7[a]	0.300	3.00	0.280	0.800	4.784×10^{-6}
8	0.300	3.78	0.280	0.803	1.126×10^{-6}
9[a]	0.310	4.50	0.280	0.900	9.054×10^{-7}
10	0.310	4.48	0.280	1.205	8.967×10^{-7}
11	0.310	4.54	0.280	1.179	8.889×10^{-7}
12	0.310	4.55	0.280	1.087	8.889×10^{-7}
13	0.310	4.55	0.280	0.993	8.888×10^{-7}
14	0.310	4.55	0.280	0.969	8.888×10^{-7}
15[a]	0.350	4.35	0.306	0.862	8.887×10^{-7}

[a] Interactive pass.

Table 4 Complete accelerometer threshold results

i	Time, s	N_i	Detection threshold, m^2/s^2	P_{FA}	P_M	Isolation threshold, m^2/s^2	P_{IS}	P_{WI}	P_{FI}
1	0	66	0.132	1.2×10^{-29}	0.051	0.085	0.996	6.7×10^{-23}	4.4×10^{-59}
2	1060	12	0.661[a]	0	0.999	0.164	0.605	5.0×10^{-31}	0
3	1252	8	0.784[a]	2.1×10^{-20}	0.999	0.185	0.399	1.6×10^{-6}	8.0×10^{-6}
4	1380	20	0.822	1.1×10^{-9}	0.990	0.176	0.385	1.2×10^{-3}	4.3×10^{-7}
5	1700	18	1.11	2.3×10^{-6}	0.990	0.219	0.227	8.7×10^{-3}	1.4×10^{-4}
6	1988	16	1.65[a]	1.1×10^{-7}	0.999	0.221	0.221	0.015	6.9×10^{-4}
7	2244	30	1.63	2.1×10^{-7}	0.251	0.359	0.954	2.8×10^{-4}	9.4×10^{-6}

$P_{VL}=8.89\times10^{-7}$

Prob [one or more false alarm during mission] $=4.9\times10^{-5}$

Prob [one or more undetected three-level failure during mission] $=1.1\times10^{-3}$

[a] At extreme of data.

Table 5 Complete gyro threshold results

i	Time, s	N_i	Detection threshold, arc-s^2	P_{FA}	P_M	Isolation threshold, arc-s^2	P_{IS}	P_{WI}	P_{FI}
1	0	3	1.0×10^{7}[a]	9.3×10^{-4}	0.999	9100	0.227	0.072	0.111
2	48	4	1.1×10^{7}[a]	8.9×10^{-4}	0.999	17,100	0.270	0.090	0.105
3	112	4	1.1×10^{7}[a]	7.3×10^{-4}	0.999	29,700	0.344	0.076	0.085
4	176	9	1.1×10^{7}[a]	5.2×10^{-4}	0.999	28,000	0.220	0.039	0.109
5	320	17	1.3×10^{7}[a]	1.7×10^{-4}	0.999	68,700	0.345	0.030	0.103
6	592	13	2.3×10^{7}[a]	1.5×10^{-7}	0.999	168,000	0.562	0.004	0.005
7	800	50	3.0×10^{7}	2.6×10^{-8}	0.999	425,000	0.715	0.003	0.019
8	1600	25	2.6×10^{7}	8.2×10^{-6}	0.900	1.10×10^{6}	0.873	1.3×10^{-5}	0.002
9	2000	30	2.8×10^{7}	8.2×10^{-5}	0.702	1.61×10^{6}	0.847	1.7×10^{-5}	0.004
10	2480	16	2.9×10^{7}	3.7×10^{-4}	0.400	3.50×10^{6}[a]	0.951	5.2×10^{-6}	1.4×10^{-4}

$P_{VL}=1.89\times10^{-5}$

Prob [one or more false alarm during mission] $=0.0251$

Prob [one or more undetected 3-level failure during mission] $=2.0\times10^{-3}$

[a] At extreme of data.

The procedure is completely analogous for gyro FDI. The final results are

$$a=5000 \text{ arc-s} \qquad b=0.2 \text{ arc-s/s}$$

$$c=91.7 \text{ arc-s} \qquad d=0.527 \text{ arc-s/s}$$

$$P_{vl}=1.89\times10^{-5}$$

Table 5 lists the complete gyro results.

Discussion

Many threshold determination techniques are based on consideration of only the single test performance probabilities or decision function statistics. Cost functions chosen on such a basis are not as directly related to the ultimate objective of a FDI system as the cost P_{vl} that is suggested in this paper. One of the most frequently used methods of this type involves the use of Monte Carlo simulation or covariance analysis of a normal system to find the statistics of the decision functions in the normal mode and then the choice as the threshold of a value three times as large as the time-varying standard deviation of the decision function (the 3σ technique).[8,9] This technique yields a value of 0.0026 for the false alarm probability on each test. Setting the thresholds to this value and using the Markov model described herein, the resulting P_{vl} for the Shuttle entry mission considered here is 1.4×10^{-4}. This value is one order of magnitude higher than the gyro P_{vl}

of the preceding section and more than two orders of magnitude higher than the corresponding accelerometer P_{vl}. The primary reason for the difference is that the probability of the occurrence of at least one detection false alarm during the mission, which includes 170 FDI tests, is 0.358 for the 3σ threshold compared to 0.0251 for gyros and 1.85×10^{-4} for accelerometers using the Markov-derived thresholds.

The comparison of results above points out several advantages of the method described here. Obviously, a performance improvement in the sense of a reduced P_{vl} is obtained for the optimized thresholds relative to the performance of the standard method. Furthermore, the construction of the Markov model has made possible comparisons of the performance of any thresholds that might be suggested.

In fact, the model makes it possible to examine the sensitivity of the performance to many different parameters. Included among these are: 1) sensor failure probability, 2) number of FDI tests during the mission (related to the FDI test rate), 3) form of the threshold, 4) initial condition on the system state probabilities, and 5) statistics of the decision functions. The complete threshold determination method itself can be reapplied to find the new optimal parameters for comparison to the old or, as in the comparison above, a performance comparison can be made with relative ease by replacing the old parameters with the new in the Markov model and recomputing P_{vl}.

The Markov model itself can also be modified to reflect more complexity in the FDI system. For instance, if N-count is included in the FDI logic, it can be reflected in the model by adding more states similar to states 3A, 5A, and 5B. More states could also be added to handle systems having higher levels of redundancy. The transition probabilities might be changed to reflect other detection or isolation schemes (provided the assumption of the independence of successive tests is not violated). One drawback to the method is that no mechanism is provided for dealing with the elapsed time between the onset and detection of a failure. This is reflected in the Shuttle gyro results (Table 5) wherein the probability of miss is very high until the last subinterval of the mission, indicating that some very soft failures might not be detected until "the last minute," so to speak. Modification of the model to add substates leading from state 2 to vehicle loss as with states 3 and 5 might remedy this difficulty.

In many FDI applications, a significant proportion of the failures are either the result of a well-known hardware fault or produce a large bias magnitude (hard failures). To detect the former, self-test equipment or BITE is often used. Since BITE tests are independent of the software FDI algorithm, the transition probabilities will reflect their performance through additional terms. For hard failures, a second level of software FDI tests is usually employed at a faster rate with relatively high thresholds. In this case, the method can be modified to include both levels of tests, and the thresholds can be determined in a unified manner.

Acknowledgments

This work was supported by NASA Johnson Space Center under Contract No. NAS 9-13809.

References

[1] Potter, J.E. and Suman, M.C., "Thresholdless Redundancy Management with Arrays of Skewed Instruments," in *Integrity in Electronic Flight Control Systems,* Agardograph no. 224, April 1977, paper 15.

[2] Willsky, A.S., "A Survey of Design Methods for Failure Detection in Dynamic Systems," *Automatica,* Vol. 12, Nov. 1976, pp. 601-611.

[3] Deyst, J.J., and Deckert, J.C., "Maximum Likelihood Failure Detection Techniques Applied to the Shuttle RCS Jets," *Journal of Spacecraft and Rockets,* Vol. 13, Feb. 1976, pp. 65-74.

[4] Desai, M.N., Deckert, J.C., and Deyst, J.J., "Dual-Sensor Failure Identification Using Analytic Redundancy," *Journal of Guidance and Control,* Vol. 2, May-June 1979, pp. 213-220.

[5] Van Trees, H.L., *Detection Estimation and Modulation Theory, Part I,* Wiley and Sons, New York, 1968.

[6] Gai, E.G., Adams, M.B., and Walker, B.K., "Determination of Failure Thresholds in Hybrid Navigation," *IEEE Transactions on Aerospace and Electronic Systems,* Vol. AES-12, Nov. 1976, pp. 744-755.

[7] Gai, E., Adams, M.B., Walter, B.K., and Smestad, T., "Correction to 'Determination of Failure Thresholds in Hybrid Navigation,'" *IEEE Transactions on Aerospace and Electronic Systems,* Vol. AES-14, July 1978, pp. 696-697.

[8] Thibodeau, J.R. III, "IMU Failure Detection Thresholds for Shuttle OFT Entry Simulations," NASA JSC, Houston, Texas, Memo FM83 (75-128), April 1975.

[9] Rich, T.M., "Initial FDI Thresholds and Results of the New IMU RM Baseline for Entry OFT 1," McDonnell-Douglas TSC, Houston, Texas, working paper E914-8A/B-018, Jan. 1977.

[10] O'Hern, E.A., "A Mathematical Model for Reliability Trade Studies for Space Delivery System Design," *Proceedings of 25th Congress of International Astronautical Federation (IAF),* Amsterdam, The Netherlands, Sept. 1974.

[11] Howard, R.A., *Dynamic Probabilistic Systems,* Vol. I, Wiley and Sons, New York, 1971.

[12] Bryson, A.E. Jr. and Ho, Y.C., *Applied Optimal Control* (revised printing), Hemisphere, Washington, D.C., 1975.

[13] Solov, E.G. and Thibodeau, J.R. III, "Failure Detection and Isolation Methods for Redundant Gimballed Inertial Measurement Units," AIAA Paper 73-851, AIAA Guidance and Control Conference, Key Biscayne, Fla., Aug. 1973.

[14] Daly, K.C., C.S. Draper Lab., personal communcation, Dec. 1978.

[15] "Space Shuttle OFT Level C FSSR, Part D Redundancy Management," Rockwell International Space Division, Downey, Calif., Nov. 1977.